

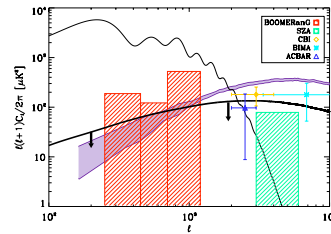
Measurement of three things in Cosmology: νI_ν (IR), A_{SZ} , f_{NL}

(since 12th Daniel Chalonge in July 2008)

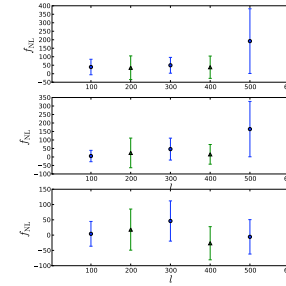
Asantha Cooray



CIBER update
(follow-up to my talk last year)

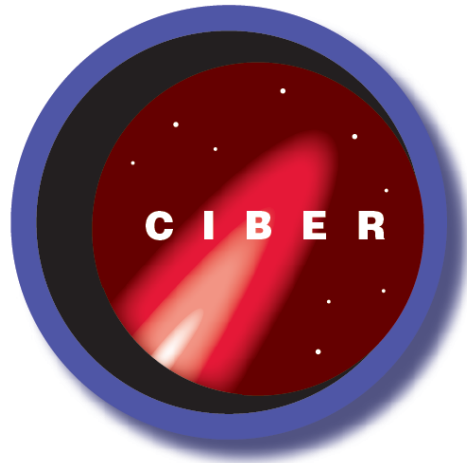


SZ with BOOMERanG



non-Gaussianity with
WMAP

A New Measurement of the Infrared Background



**The Cosmic Infrared
Background Experiment**



UC Irvine
Asantha Cooray (Co-I)
Sam Kim
Alexandre Amblard



JPL / Caltech
John Battle
Jamie Bock (PI)
Andrew Lange
Louis Levenson
Ian Sullivan
Mike Zemcov



UC San Diego
Brian Keating (Co-I)
Tom Renbarger



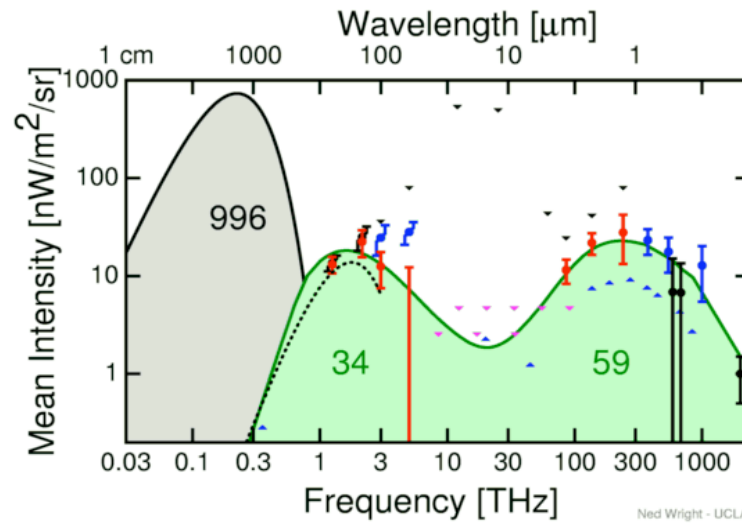
ISAS / JAXA
Toshio Matsumoto
Shuji Matsuura
Kohji Tsumura
Takehiko Wada

Nagoya U.
Mitsunobu Kawada



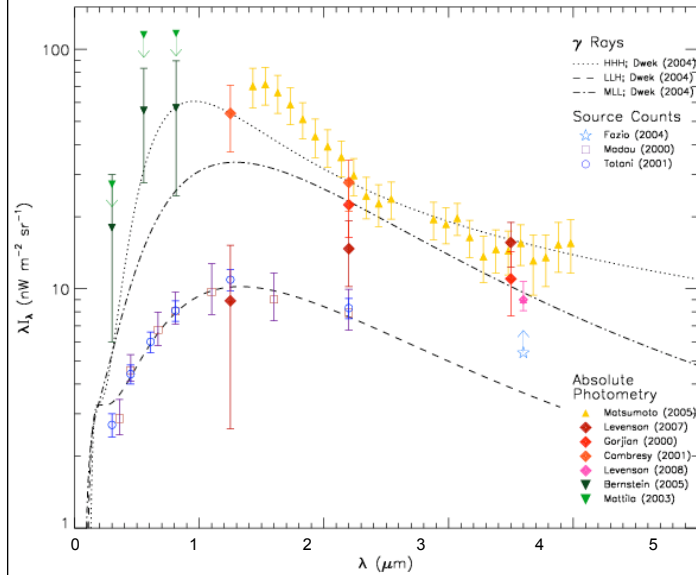
KASI
Dae-Hee Lee

What's the matter with the Infrared Background?



What is the extragalactic background light at IR wavelengths?

What's the matter with the Infrared Background?



- Large discrepancy in
Absolute photometry
vs. **Galaxy counts**
vs. **TeV blazars**

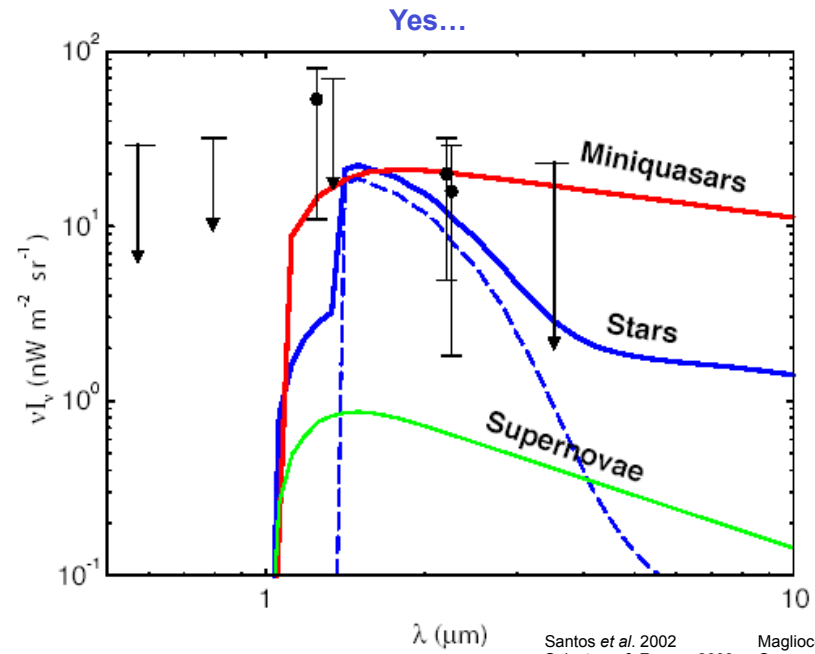
- Is this due to systematic
errors?

- or -

- Could there be a diffuse
component missed by
galaxy counts, such as
due to reionization or extra
dust components in the
Solar System or Galaxy?

What is the extragalactic background light at IR wavelengths?

The IR (DIRBE/IRTS) Excess: Could Exotic Sources Produce it?



Santos *et al.* 2002
Salvaterra & Ferrara 2003
Fernandez & Komatsu 2006

Magliocchetti *et al.* 2003
Cooray & Yoshida 2004

The IR (DIRBE/IRTS) Excess: Could Exotic Sources Produce it?

...but there are difficulties

Do not need large IRB to explain WMAP reionization optical depth:

$$\tau_e = 0.087 \pm 0.017$$

-need $n_\gamma = (1.5 \text{ to } 2) C_{\text{IGM}} (\tau_e / 0.09)$ [γ /baryon]

-while IRTS excess at H-band: $n_\gamma = f_{\text{esc}} (1+z) u_J / 0.7 E_a n_b \sim 2500 f_{\text{esc}}$

Population III Stars

-Must convert 5-10 % of Baryons into Pop III stars

High star formation fraction in collapsed structures

Many recombinations to suppress Ly continuum

-Hard to avoid metal overproduction

Stars between 140 – 260 solar masses give

PISN, eject half the star's mass in metals

Mini-Quasars

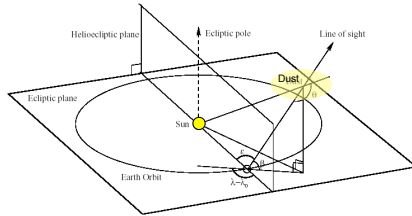
-Need $1/5000^{\text{th}}$ the formation rate of Pop III stars, but

Overproduce SXB unless very X-ray quiet

Exceed current estimated black hole densities

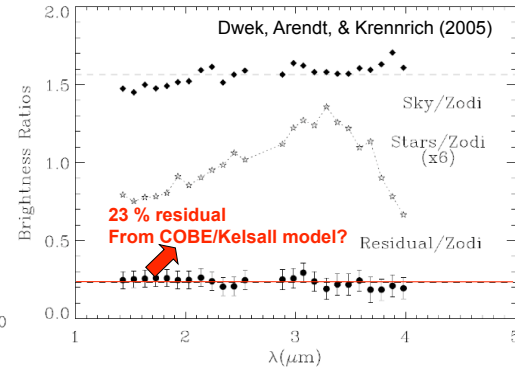
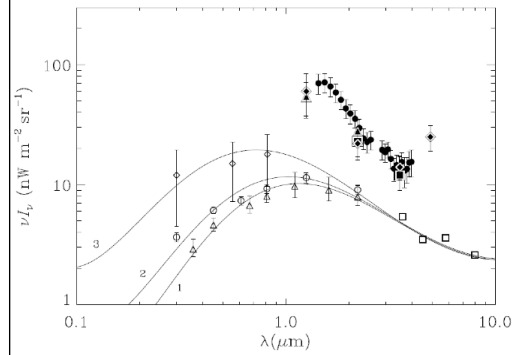
Madau & Silk 2004

Is the DIRBE/IRTS excess a Zodiacal Light Residual?

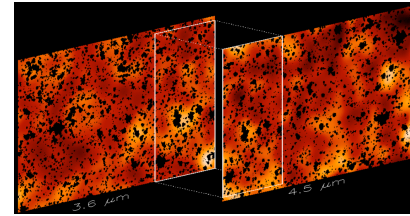
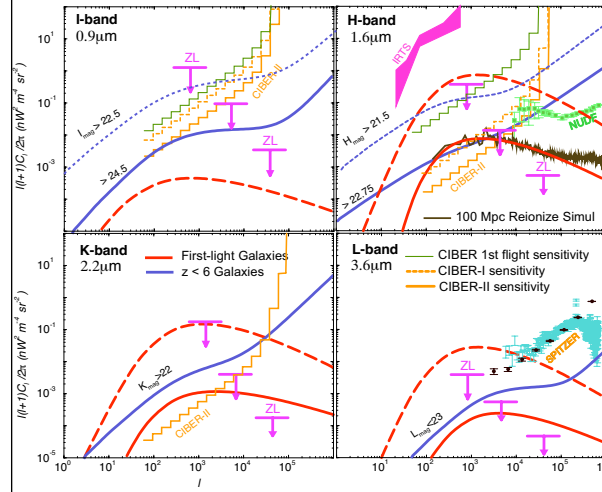


Zodiacal Light is just scattered sunlight

DIRBE team used a multi-component model (aka Kelsall model, but model may undercount scattered zodi)



However, excess IR Background Fluctuations have been Detected

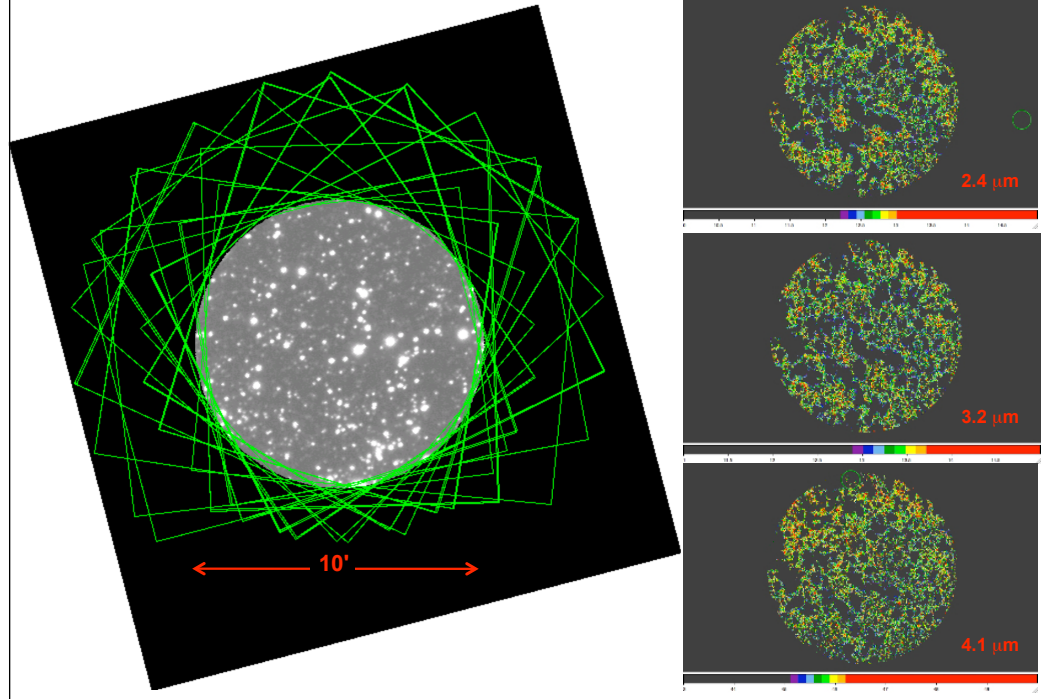


- **First detection reported by Kashlinsky *et al.* 2005**, Nature 438 with Spitzer at 3.5 and 4.5 μm Interpreted as evidence for a $z > 8$ first-light component responsible for reionization (also Kashlinsky *et al.* 2006 with GOODS)

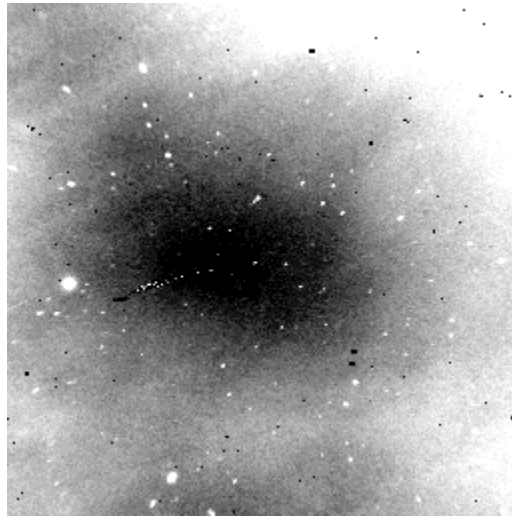
- **Could it be partly due to undetected dwarf galaxies at moderate redshifts of 1 to 3** (Cooray *et al.* 2006; Chary *et al.* 2008 using fluctuations in GOODS and a stacking analysis on multi-wavelength ACS data; Of course, Kashlinsky disagrees with this suggestion. *However, fluctuations as $z > 8$ only inconsistent with $z \sim 6$, 7 UV LFs; Chary & Cooray in prep*)

- **Thompson *et al.* 2007 report upper limits** with HST/ NICMOS, which are argued to be inconsistent with Kashlinsky interpretation for $z > 8$ sources

Akari Background Fluctuations Coming Soon!



The Case for Space



Airglow Emission

- Atmosphere is **500 – 2500** times brighter than the astrophysical sky at 1-2 μm
- Airglow fluctuations in a **1-degree** patch are **10^6** times brighter than CIBER's sensitivity in 50 s
- Brightest airglow layer at an altitude of **100 km...** can't even use a balloon

H-band $9^\circ \times 9^\circ$ image over 45 minutes from Kitt Peak

Wide-field airglow experiment: <http://pegasus.phast.umass.edu/2mass/teaminfo/airglow.html>

How can a rocket experiment compete with these?

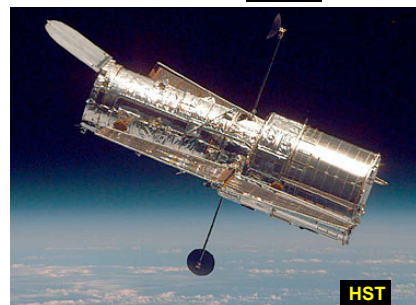
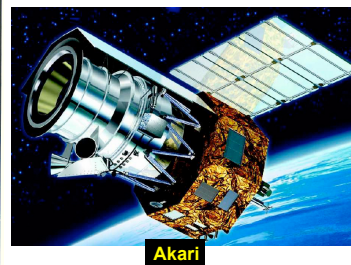
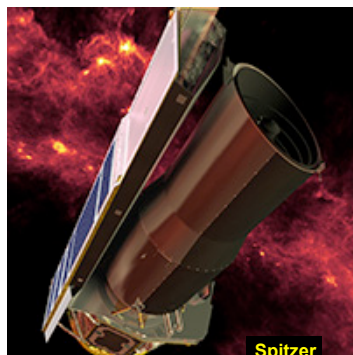


Table 5.2 Comparison with Existing Instruments

Instrument	Bands [μm]	FOV	Sub-fields	Etendue
CIBER2	0.6, 0.9, 1.4, 2.1	85' x 85'	1	1
CIBER1	0.9, 1.6	120' x 120'	1	0.1
NICMOS	1.1, 1.6, 2.1	1' x 1'	9900	0.002
WFC3	0.6, 1.0, 1.4, 1.6	2' x 2'	1500	0.01
Akari	2.3, 3.2, 4.1	12' x 12'	50	0.02
Spitzer	3.6, 4.5	5' x 5'	270	0.01

Notes: Etendue = Area x Ω x Simultaneous Bands

Sub-fields = number of pointings to cover 2 sq. degrees

Features about the Sounding Rocket Program

Flights are short

Apogee ~ 320 km for Terrier Black-Brant
Useful science time ~ 300 s

May have longer flights in the future

600 km and 600 s for Talso-Terrier-Nihka-Brant, no recovery
12hr-24hr “orbital” sounding rocket being discussed

Unique Capabilities

No atmosphere, cold optics → specialized instruments

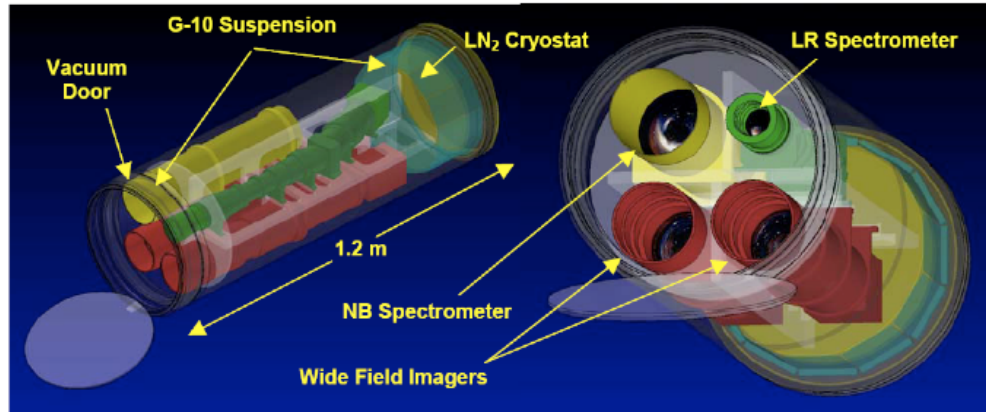
Developed sub-systems provided

Custom attitude control system points to < 2°
Telemetry system provides 30 Mbps
Wide range of available launch sites
(4 sites in US+Alaska; Marshall Islands in South Pacific)

Programs can be small

CIBER NASA APRA proposal costs = \$1M in total
(With 2 1024² and 2 256² arrays, that's 45¢ per pixel)
supports research of 2 graduate students, 1.5 postdocs

CIBER Science Goals



Dual Wide-Field Imagers
 $\lambda = 0.8 \mu\text{m} \text{ \& } 1.6 \mu\text{m}$ $\lambda/\Delta\lambda = 2$
 $2^\circ \times 2^\circ \text{ FOV}$ $7'' \text{ pixels}$

- Measure power spectrum from $7''$ to 2 degrees

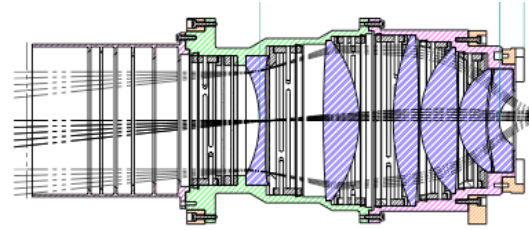
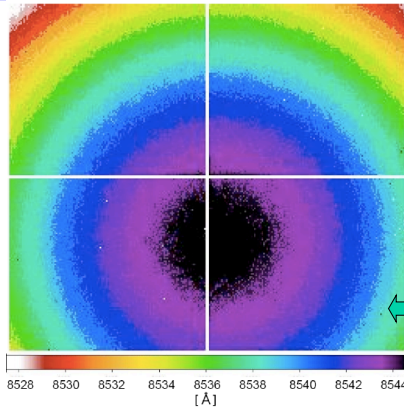
Low-Resolution Spectrometer
 $\lambda = 0.8 - 2.0 \mu\text{m}$ $\lambda/\Delta\lambda \sim 20$
 $4^\circ \times 4^\circ \text{ FOV}$ $60''$
 pixels

- Search for Ly cutoff feature in $0.8 - 1.2 \mu\text{m}$ region

Narrow-Band Spectrometer
 $\lambda = 0.8542 \mu\text{m}$ $\lambda/\Delta\lambda = 1000$
 $8^\circ \times 8^\circ \text{ FOV}$ $120''$
 pixels

- Use Fraunhofer lines to measure absolute Zodiacal intensity

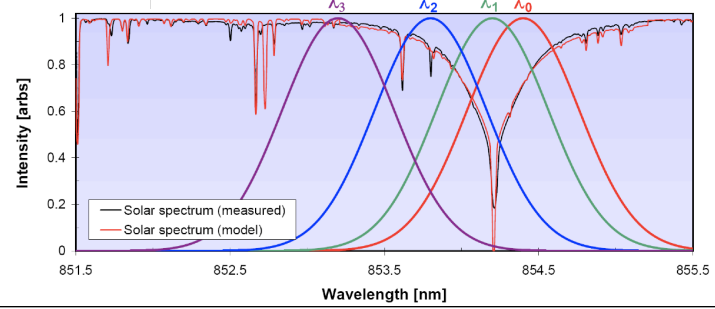
Narrow-Band Spectrometer



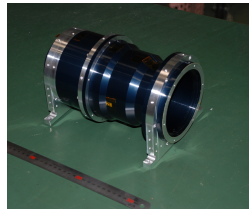
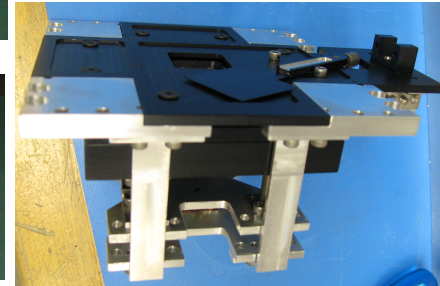
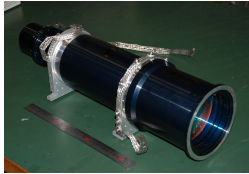
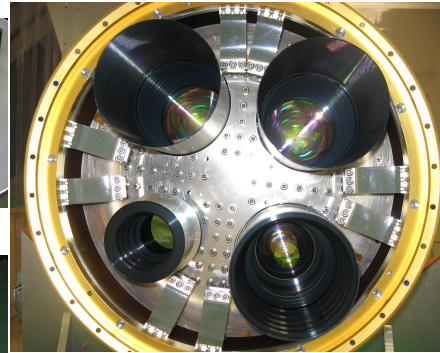
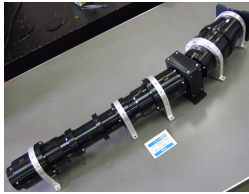
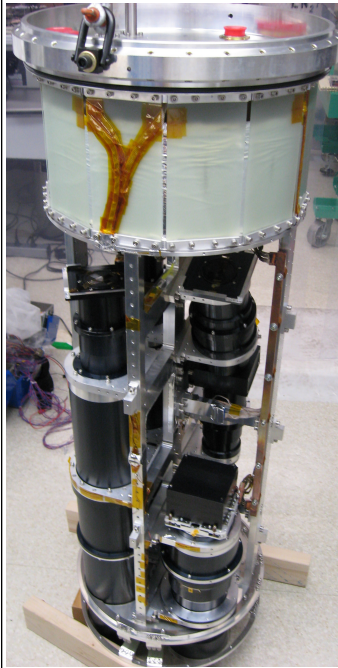
NIST calibration data
 $I(\text{photo}) \sim 30 \text{ e-/s}$

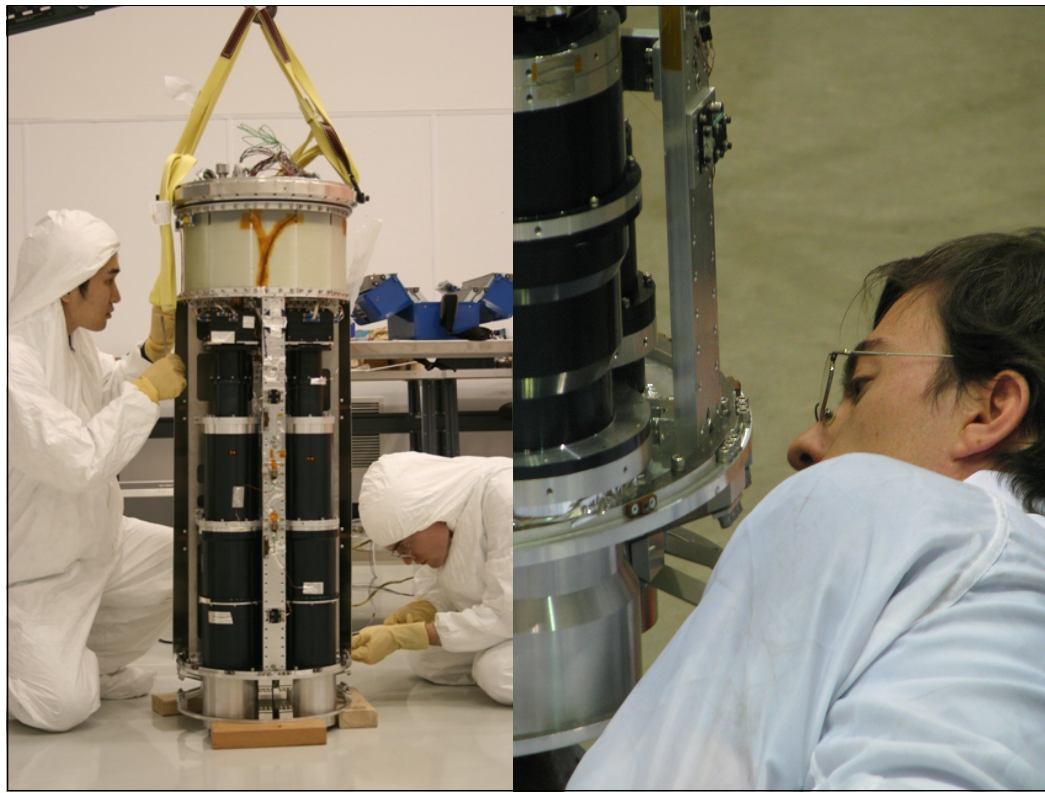
Science Goal:
Measure Fraunhofer
Ca II 854.2 nm line
EW to 1 % absolute

Solar Spectrum and Fraunhofer Lines

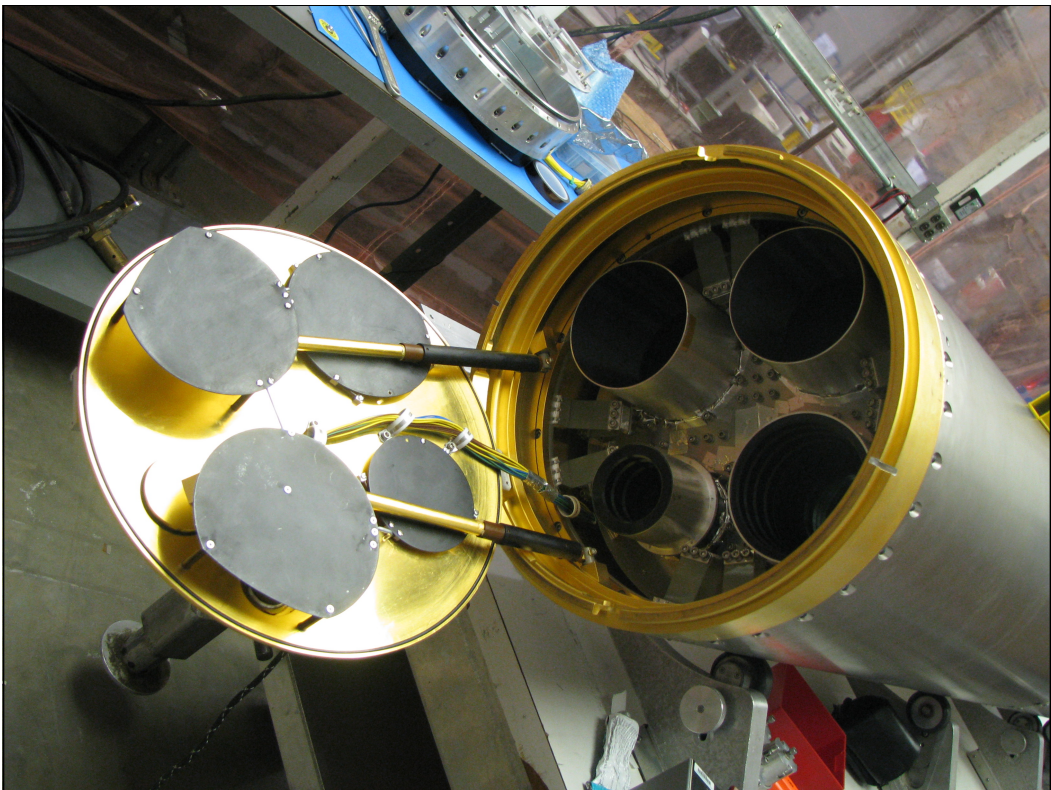


CIBER Hardware







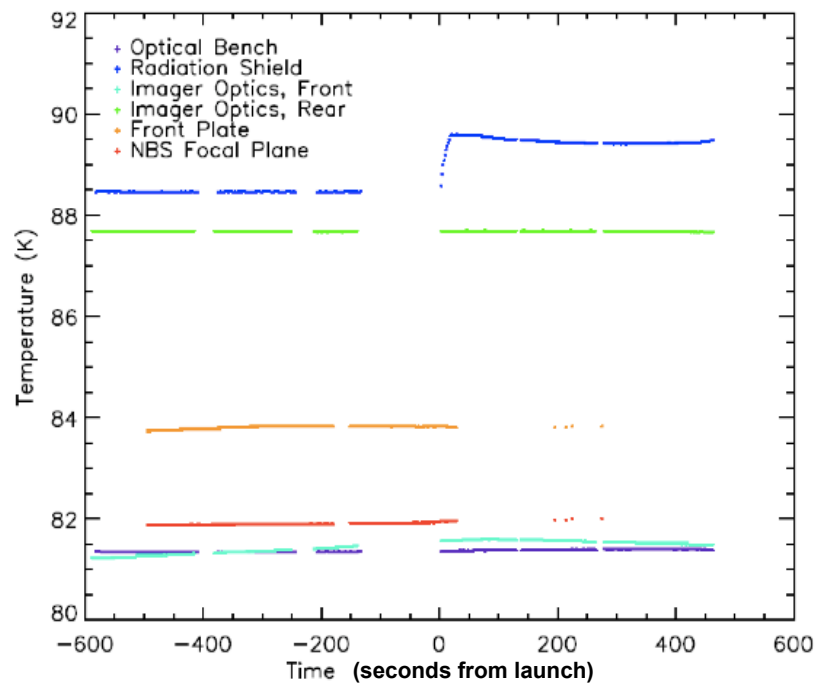




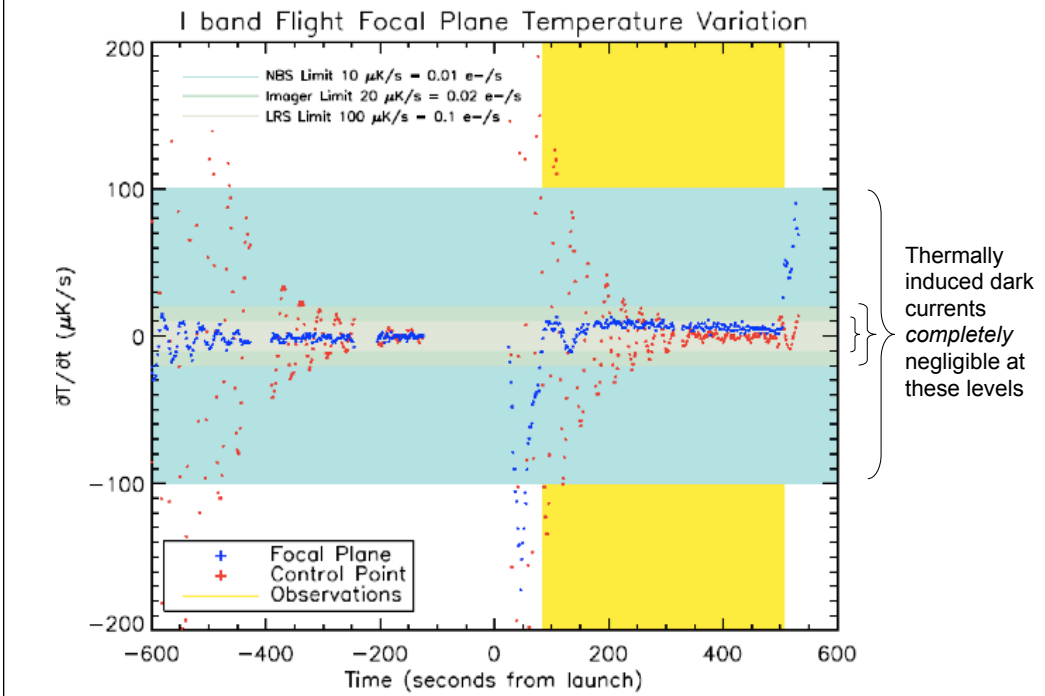




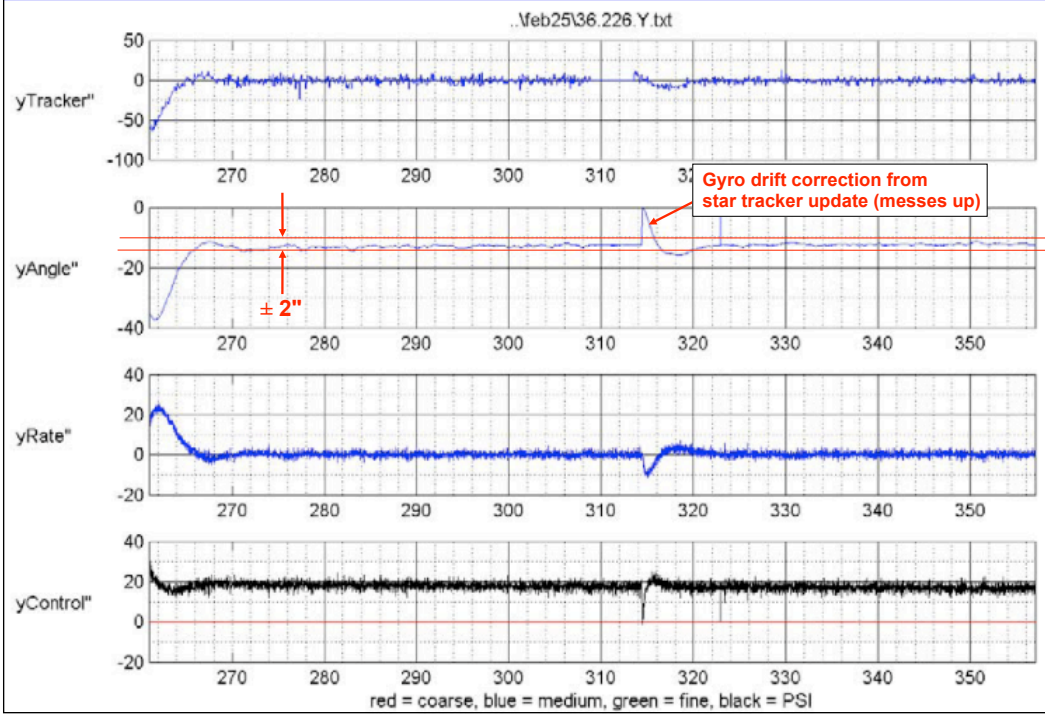
Temperatures in Flight



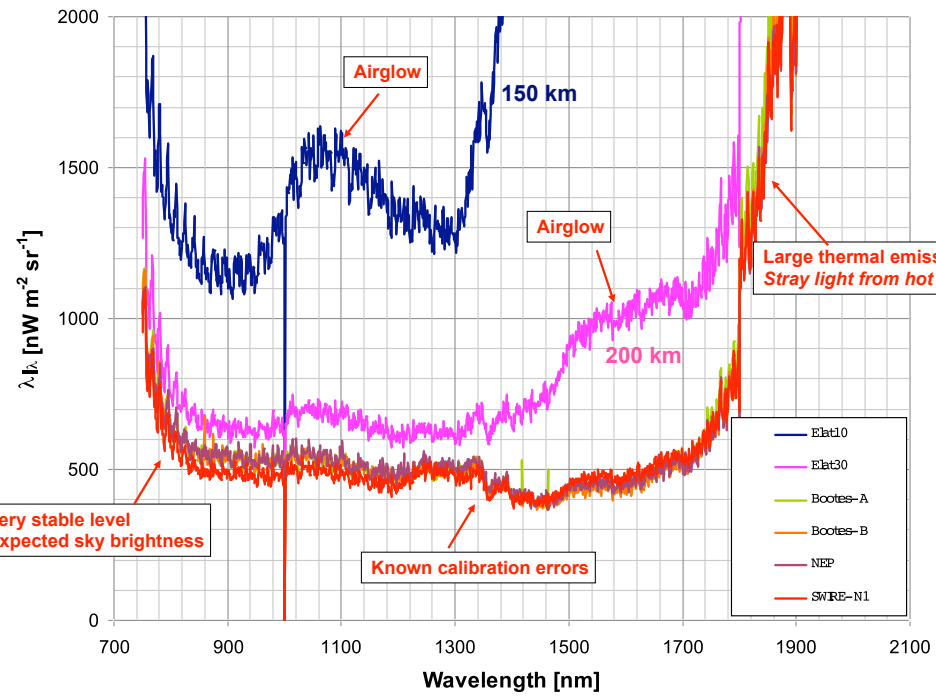
Precision Thermometry & Control of Focal Plane



Attitude Control System Performance

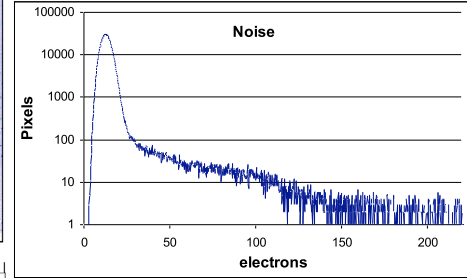
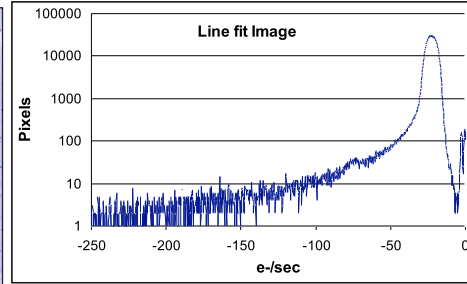
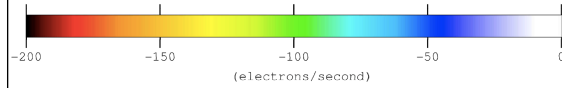
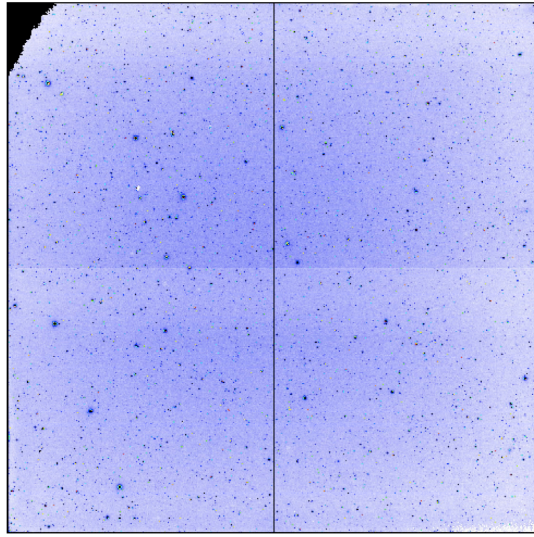


Preliminary LRS Spectra



Preliminary 0.9 μm Imager Data

I-band Imager



Median photocurrent = 22 e-/s
Median read noise = 12.6 e-



Nosecone!



CIBER History

CIBER-I launched successfully February 25, 2009

First flight constituted a test flight of the instrument (similar to North American test flights of CMB balloon experiments), but adequate science data!

Second flight this fall (date TBD; September 2009-January 2010)

CIBER-I first flight science papers now in preparation

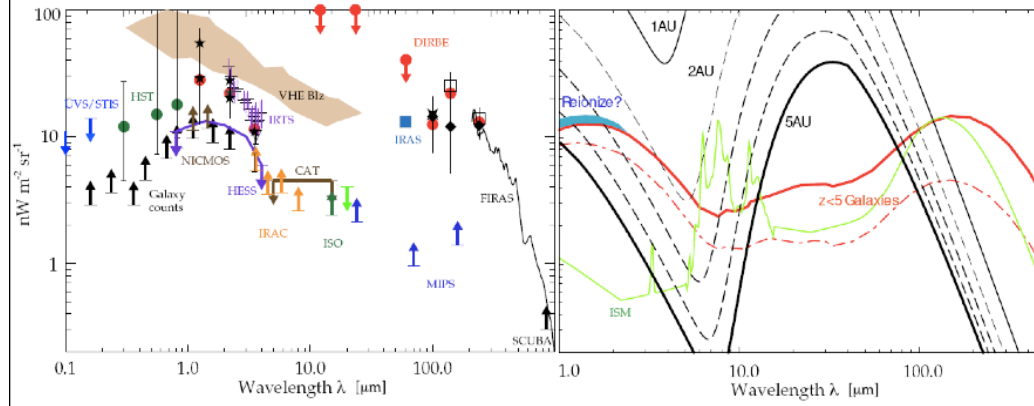
(2 papers planned. One on EBL and one on zodi. CIBER is the first experiment to do a spectral study of the EBL and zodi between 0.6 and ~2 microns!)

CIBER-I will fly a total of 4 times. Last flight in fall/winter 2010 will be long duration with a launch from Alaska (payload in Pacific ocean, not recovered).

An upgraded CIBER-II with 2048x2048 arrays was recently proposed to NASA APRA for flights starting fall 2012.

Beyond CIBER: Exo-Zodiacal EBL Explorer?

Cooray et al. 2009, *A New Era in Extragalactic Background Light Measurements, White paper to Astro2010 Decadal Survey*,
arXiv.org:0902.2372



Small instrument attached to an outer (\geq Jupiter) planets mission

- support from planetary community
- could be cheap/small/simple
- upcoming Discovery program opportunity to Europa.

**A search for sub-degree SZ fluctuations
with multi-frequency BOOMERanG-2003
CMB data**

Marcella Veneziani, Alexandre Amblard, Paolo Serra, AC



& the BOOMERanG/Pol 03 Collaboration

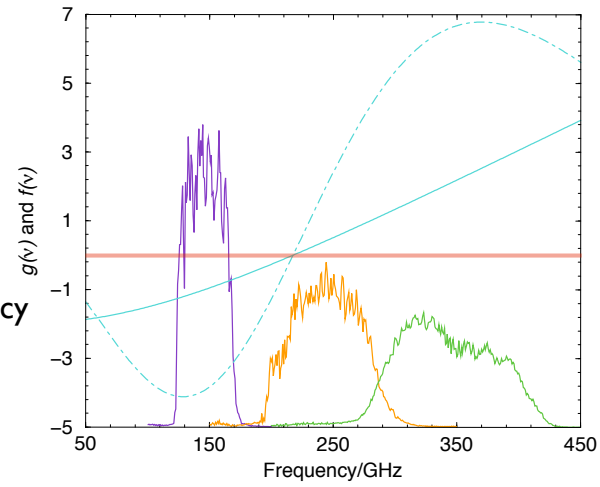
arxiv:0904.4313 (in press ApJL)

SZ effects

SZ effects:

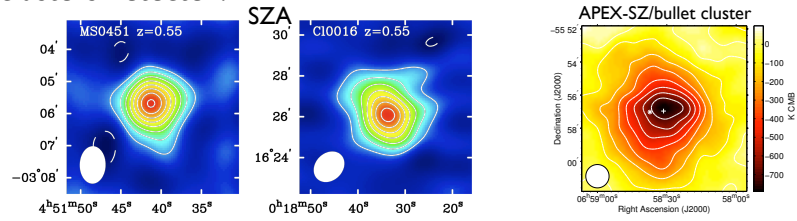
- ❖ Thermal SZ
- ❖ Kinetic SZ

BOOMERanG frequency coverage is well suited to measure Thermal SZ.

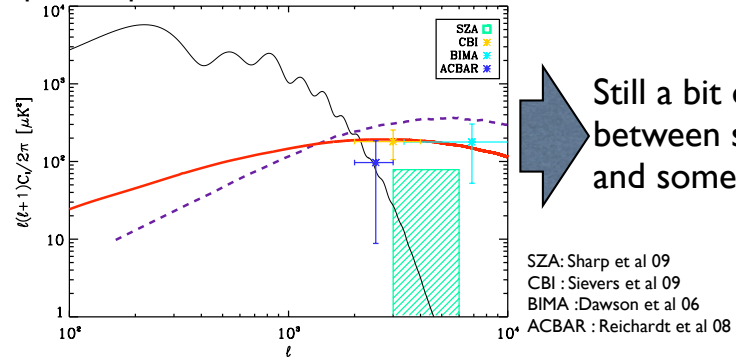


Where we are right now.

Some clusters detected:

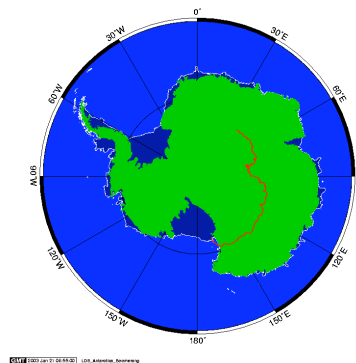
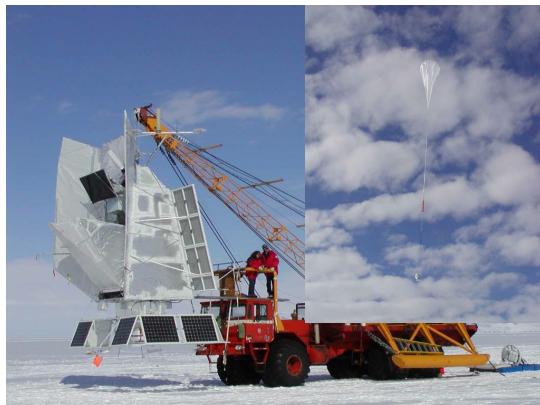


a power spectrum :



BOOMERanG 2003

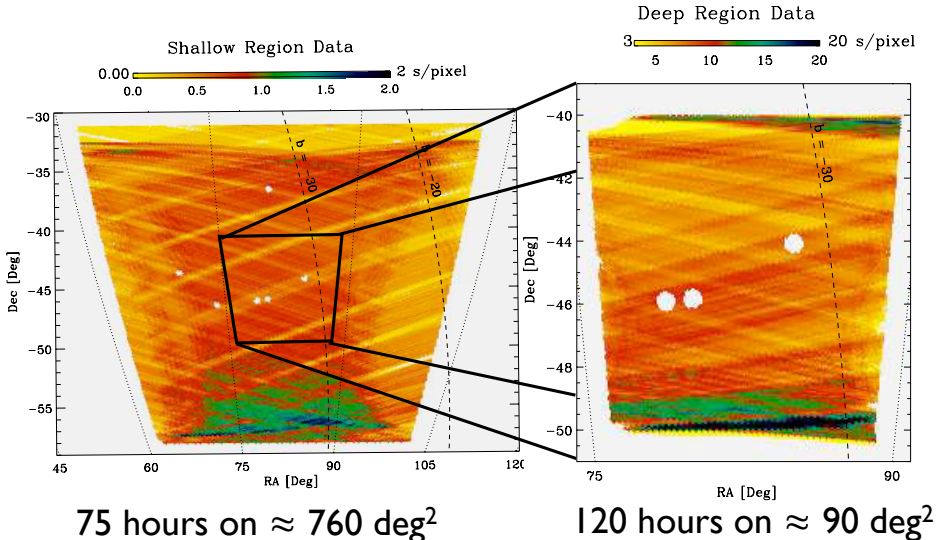
Launch January 6th 2003 05:00 UT, terminated on January 21st 06:59

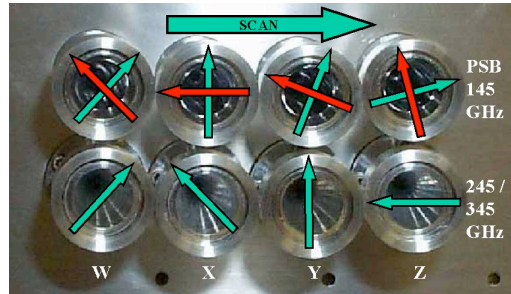


311 hours of data spent on 3 fields :

- ❖ 75 hours on a shallow field
- ❖ 120 hours on a deep field
- ❖ 30 hours over the Galactic plane

BOOMERanG 2003

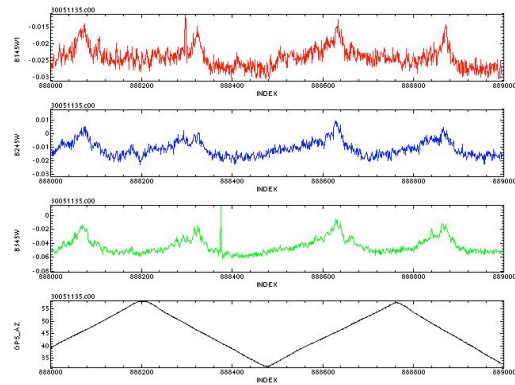




- ❖ Total number of detectors :
 8 bolometers @ 145 GHz
 4 bolometers @ 245 GHz
 4 bolometers @ 345 GHz

- ❖ Removed 2 detectors previously known for high noise (Masi et al 06):
 245X and 345Z

- ❖ Removed 2 detectors, we found have higher noise:
 145Z2 and 345Y



- 7 bolometers @ 145 GHz
 3 bolometers @ 245 GHz
 2 bolometers @ 345 GHz

The Data Set

For the 3.4' pixel deep region :

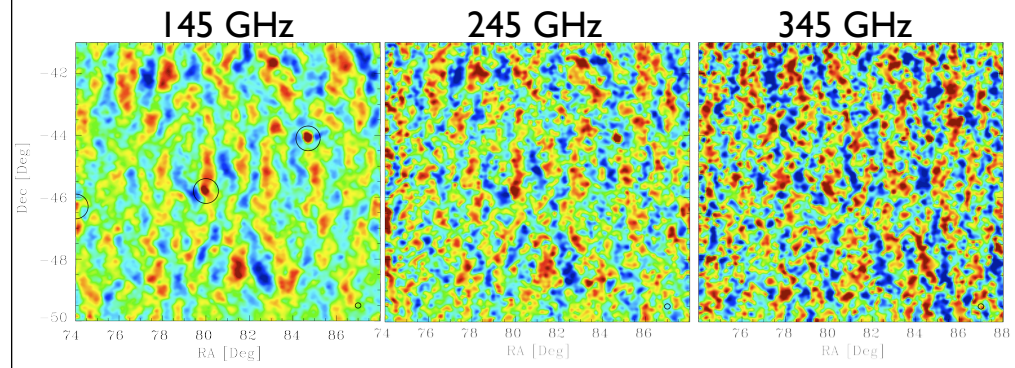
B03 INSTRUMENT SUMMARY

$\langle \nu \rangle$ GHz	$\frac{\text{MJy/sr}}{\text{K}_{\text{CMB}}}$	θ_{phys} FWHM	θ_{eff}^a FWHM	NET ^b $\mu\text{K}_{\text{CMB}}\sqrt{s}$	σ_{pix}^c μK_{CMB}	$s(\nu)=$ $g(\nu)/g(\nu_{RJ})$
145	388	9.95'	11.5'	63	18	0.5
245	462	6.22'	8.5'	161	50	-0.2
345	322	6.90'	9.1'	233	72	-1.0

Beams allow to go up to $l \sim 1200$

Calibration error 2, 8, 13 % @ 145, 245, 345 GHz

BOOMERanG03 maps



Trace of CMB, dust and radio sources.

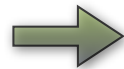
Isolating the SZ

Given a number of frequencies, one can use an internal linear combination to keep a specific source (Tegmark et al 96, Tegmark et al 03):

$$a_{lm} = \sum_{freq=i} w_l^i a_{lm}^i \quad \mathbf{w}_l = \frac{\mathcal{C}^{-1} \mathbf{e}}{\mathbf{e}^T \mathcal{C}^{-1} \mathbf{e}}$$

Combining the different frequencies with the "optimal" weights :

$$\mathcal{C}_{SZ} = \mathbf{w}^T \mathcal{C} \mathbf{w}$$



Minimize the total variance : signal + noise

More aggressive foregrounds subtraction

We used only cross-spectra to minimize primarily the “foreground” residuals, not the noise and divided by $s(\nu_i)$ (Cooray et al 00):

$$C_{ij} = \sum_{l \in b, m} \sum_{u, v} \frac{\langle a_{lm}^{i, u} a_{lm}^{j, v*} \rangle}{s(\nu_i) s(\nu_j) b_l^{i, u} b_l^{j, v}} \quad \text{with } u \neq v, \text{ if } i = j$$

$s(\nu)$: SZ frequency spectrum

b_l : beam function

i, j : indices of the frequency

u, v : indices of the detector

145-145 GHz : 21 pairs

145-245 GHz : 21 pairs

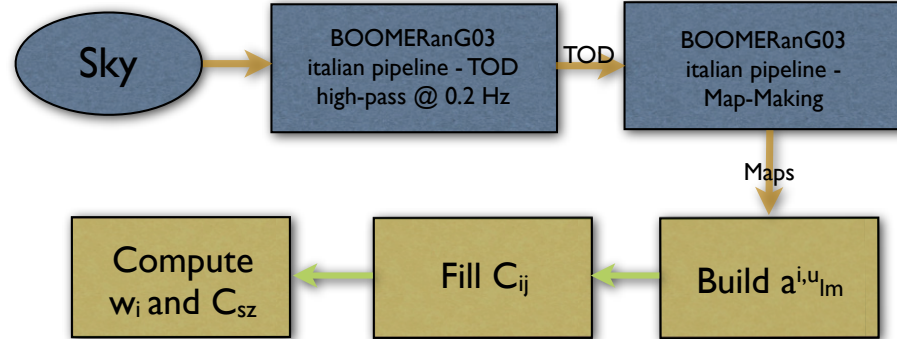
145-345 GHz : 14 pairs

245-245 GHz : 3 pairs

245-345 GHz : 6 pairs

345-345 GHz : 1 pair

Analysis Roadmap



Preliminary Result

SZ POWER SPECTRUM ESTIMATES			
ℓ -range	bin 1	bin 2	bin 3
	250-450	450-700	700-1200
Optimal weights			
$w_{145\text{GHz}}$	0.9323	0.8514	0.7289
$w_{245\text{GHz}}$	0.4193	0.3771	0.3002
$w_{345\text{GHz}}$	-0.3515	-0.2285	-0.0292
Raw SZ	236	164	538

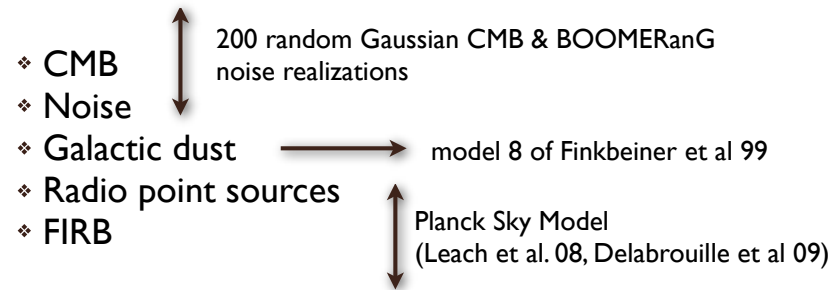
w_{145}/s_{145}	1.88	1.71	1.47
w_{245}/s_{245}	-1.94	-1.74	-1.39
w_{345}/s_{345}	0.35	0.22	0.03



Not all CMB is removed and
other residuals might be there
+ no error estimate
We Need Simulations

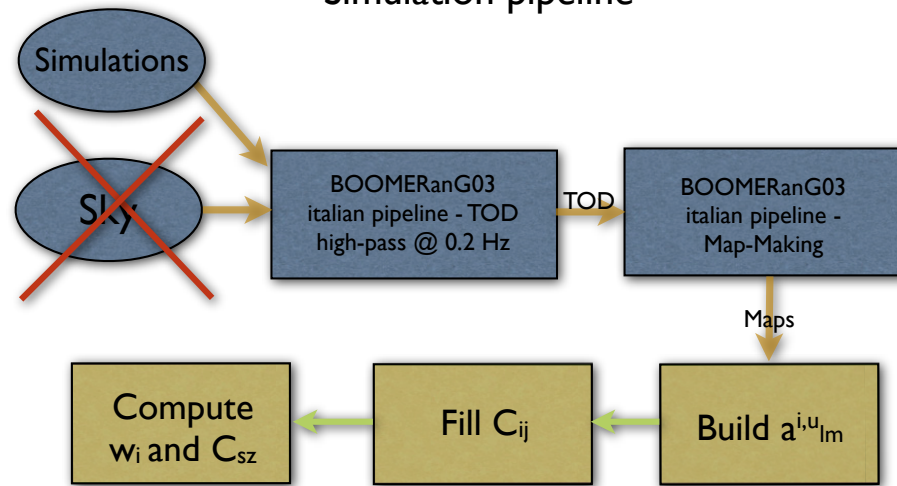
Simulations

We included the following emissions :



We used 1 set of simulations with the predictions from these models.

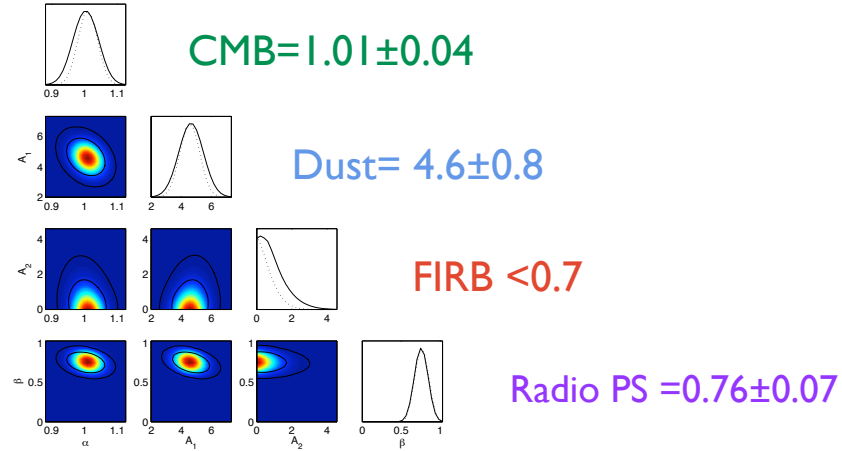
Simulation pipeline



Each simulation goes through the complete pipeline.

Fitting our “Foreground” templates

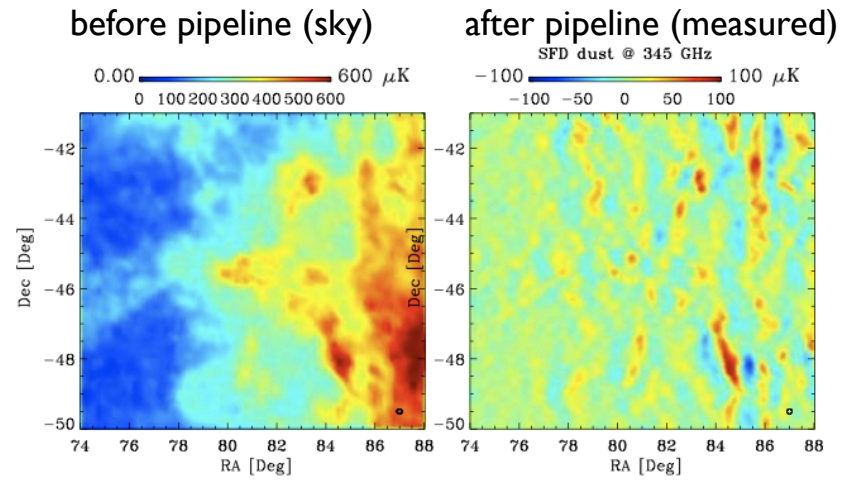
$$C_l^{\text{data}} = p_{\text{cmb}} \times C_l^{\text{cmb}} + p_{\text{dust}} \times C_l^{\text{dust}} + p_{\text{radio}} \times C_l^{\text{radio}} + p_{\text{FIRB}} \times C_l^{\text{FIRB}}$$



Two more sets :

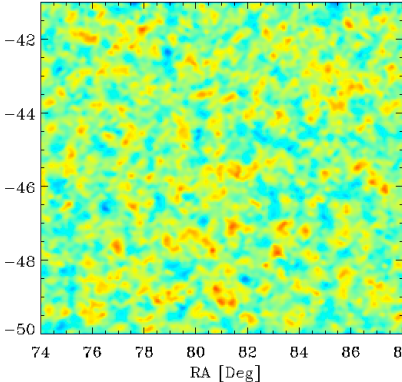
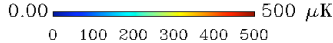
- ❖ $p_{\text{cmb}}=1, p_{\text{dust}}=4.6, p_{\text{radio}}=0.76, p_{\text{FIRB}}=0.7$
- ❖ $p_{\text{cmb}}=1, p_{\text{dust}}=4.6, p_{\text{radio}}=0.76, p_{\text{FIRB}}=0.0$

Dust at 345 GHz

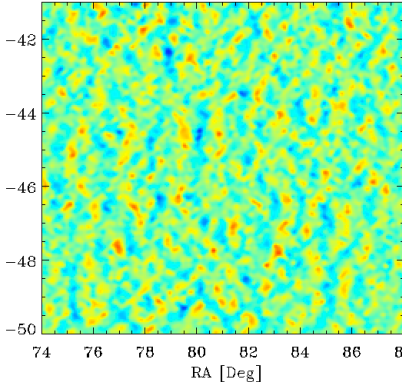


FIRB at 345 GHz

before pipeline (sky)

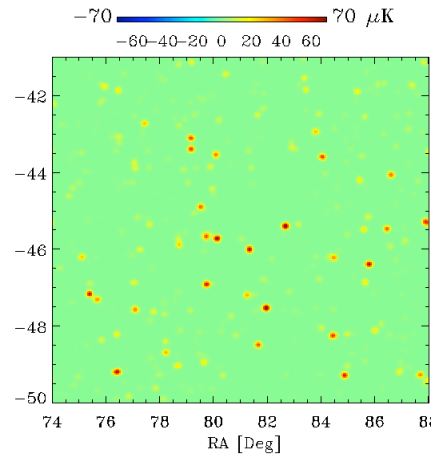


after pipeline (measured)

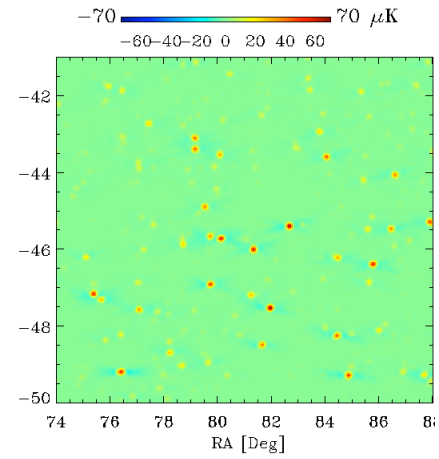


Radio PS at 145 GHz

before pipeline (sky)



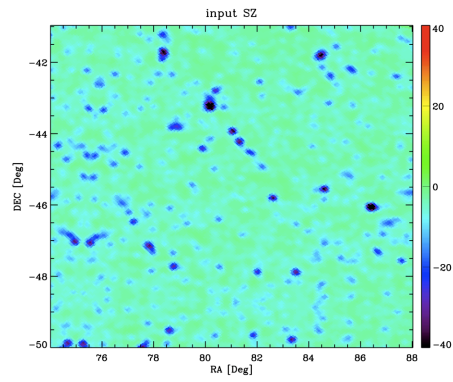
after pipeline (measured)



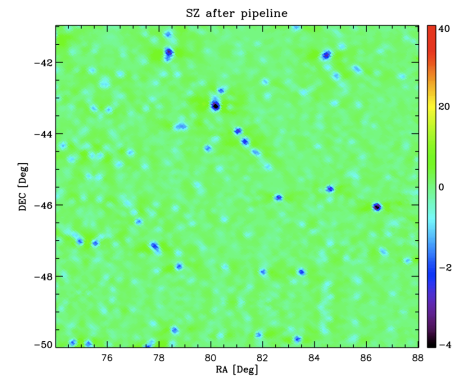
SZ at 145 GHz

(from White 03*)

before pipeline (sky)



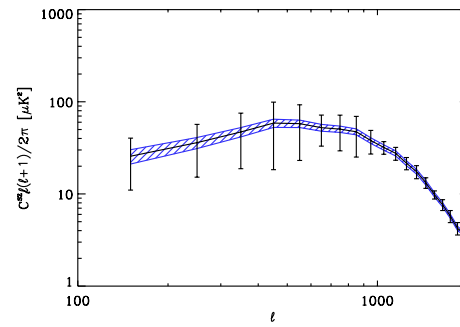
after pipeline (measured)



*<http://mwhite.berkeley.edu/tSZ/PlanckSZ/>

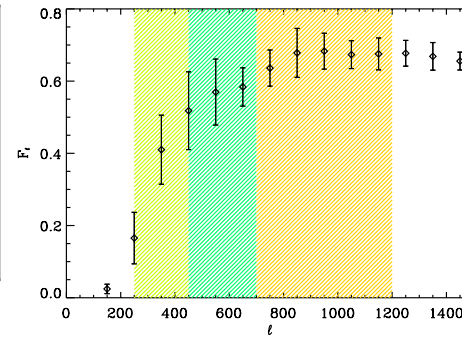
SZ filtering

Power spectra of 10 SZ simulations



SZ variance 2-6 times larger than
Gaussian CV

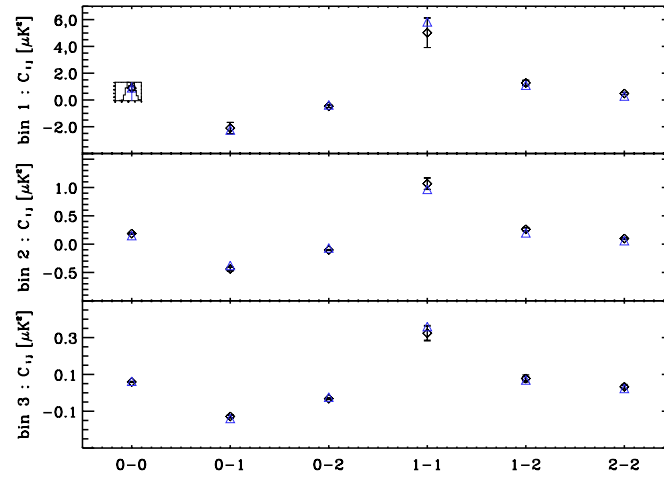
SZ transfer function for BOOMERanG
scan-strategy and filtering

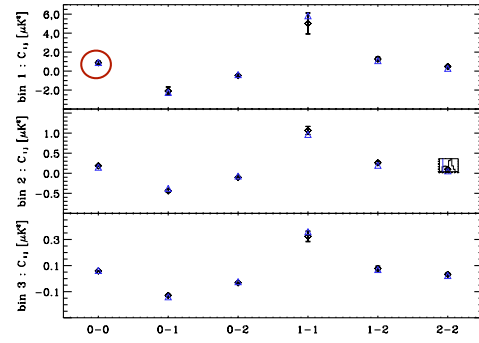
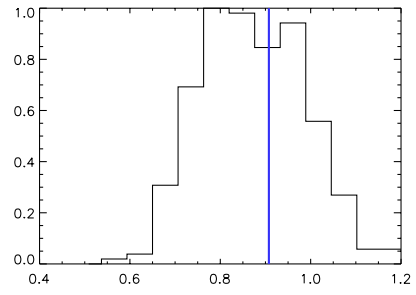


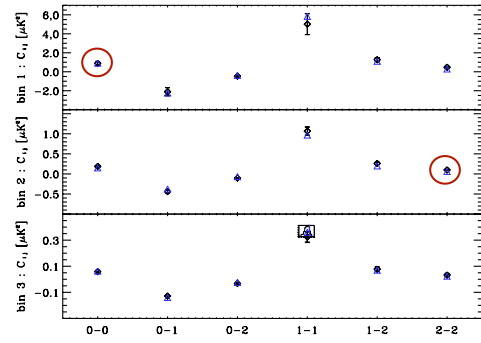
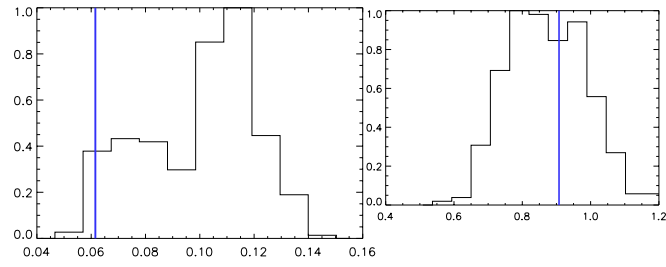
$F_0 = 0.5 \pm 0.1$ (20%)
 $F_1 = 0.6 \pm 0.05$ (8.3%)
 $F_2 = 0.7 \pm 0.04$ (5.7%)

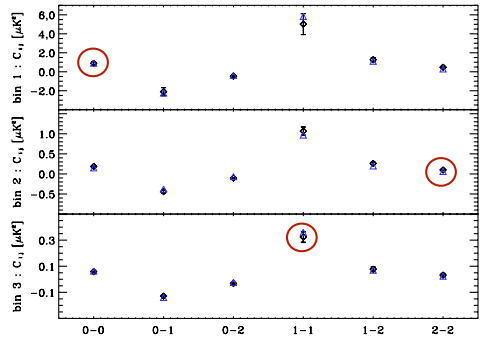
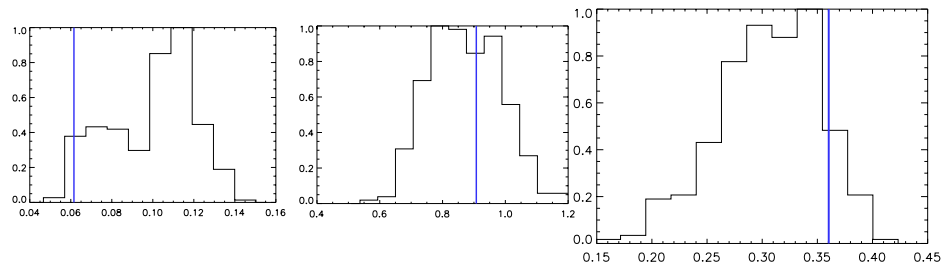
Some data/simulations comparison

$$C_{ij} = \sum_{l \in b, m} \sum_{u, v} \frac{\langle a_{lm}^{i,u} a_{lm}^{j,v*} \rangle}{s(\nu_i) s(\nu_j) b_l^{i,u} b_l^{j,v}} \quad \text{with } u \neq v, \text{ if } i = j$$





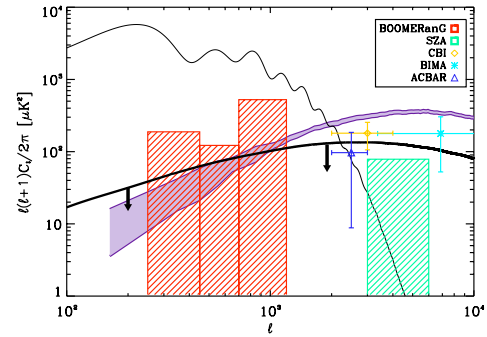




Results

SZ POWER SPECTRUM ESTIMATES

	bin 1	bin 2	bin 3
ℓ -range	250-450	450-700	700-1200
Optimal weights			
$w_{145\text{GHz}}$	0.9323	0.8514	0.7289
$w_{245\text{GHz}}$	0.4193	0.3771	0.3002
$w_{345\text{GHz}}$	-0.3515	-0.2285	-0.0292
Raw SZ	236	164	538
Residuals ^(a)			
CMB	53	36	70
Instr. noise	92	12	-95
Galactic dust	68	82	138
FIRB	44	81	195
Radio sources	3	7	58
Total residual	247	202	338
SZ Band Power Uncertainties ^(b)			
Instr. noise	154	116	280
Foregrounds	37	79	145
Beam	3	5	44
Calibration	121	77	63
Transfer func.	2	3	11
Cosmic & NG Var ^(c)	7	6	4
Final SZ Band Power	-11 ± 199	-38 ± 160	200 ± 325



The combined limit from BOOMERanG
is $< 234 \mu\text{K}^2$ at 2σ
BOOMERanG alone $\sigma_{8(\text{SZ})} < 1.14$ at 95%
confidence

Combined constrains give $\sigma_{8(\text{SZ})} < 0.95$ at 95% confidence

A_{SZ} : Conclusions

- ❖ We put a first limit of $234 \mu\text{K}^2$ (2σ) on SZ emission at sub-degree scales between l of 250 and 1200. BOOMERanG is the only experiment that can constrain at these large angular scales
- ❖ Major uncertainty come from FIRB and high noise at 345 GHz
- ❖ Planck should be able to do better with more frequencies and improved sensitivity, but FIRB will be the dominant confusion for a high signal-to-noise detection with Planck alone.
- ❖ Planck + Herschel (especially over the combined ~ 600 -1000 deg^2 of Herschel-ATLAS will allow SZ and FIRB separation).

A Measurement of Primordial Non-Gaussianity using WMAP 5-year Temperature Skewness Power Spectrum

Joseph Smidt, Alexandre Amblard, Paolo Serra, AC



arxiv:0907.4051 out today
(PRD to be submitted)

$$\Phi(\mathbf{x}) = \phi_L(\mathbf{x}) + f_{\text{NL}} [\phi_L^2(\mathbf{x}) - \langle \phi_L(\mathbf{x}) \rangle^2]$$

Detection of primordial non-Gaussianity (f_{NL}) in the WMAP 3-year data at above 99.5% confidence

Amit P. S. Yadav¹ and Benjamin D. Wandelt^{1,2}

¹Department of Astronomy, University of Illinois at Urbana-Champaign, 1002 W. Green Street, Urbana, IL 61801 and
²Department of Physics, University of Illinois at Urbana-Champaign, 1110 W. Green Street, Urbana, IL 61801

We present evidence for the detection of primordial non-Gaussianity of the local type (f_{NL}), using the temperature information of the Cosmic Microwave Background (CMB) from the WMAP 3-year data. We employ the bispectrum estimator of non-Gaussianity described in [1] which allows us to analyze the entirety of the WMAP data without an arbitrary cut-off in angular scale. Using the combined information from WMAP's two main science channels up to $l_{\text{max}} = 750$ and the conservative Kp0 foreground mask, we find $27 < f_{\text{NL}} < 147$ at 95% C.L., with a central value of $f_{\text{NL}} = 87$. This corresponds to a rejection of $f_{\text{NL}} = 0$ at more than 99.5% significance. We find that this detection is robust to variations in l_{max} , frequency and masks, and that no known foreground, instrument systematic, or secondary anisotropy explains our signal while passing our suite of tests. We explore the impact of several analysis choices on the stated significance and find 2.5σ for the most conservative view. We conclude that the WMAP 3-year data disfavors canonical single field slow-roll inflation.

WMAP 3-year data: 87 +/- 30
(Yadav & Wandelt)

TABLE 5
CLEAN-MAP ESTIMATES AND THE CORRESPONDING 68% INTERVALS OF THE LOCAL FORM OF PRIMORDIAL NON-GAUSSIANITY, $f_{\text{NL}}^{\text{local}}$, THE POINT SOURCE BISPECTRUM AMPLITUDE, b_{src} (IN UNITS OF $10^{-5} \mu\text{K}^2 \text{sr}^2$), AND MONTE-CARLO ESTIMATES OF BIAS DUE TO POINT SOURCES, $\Delta f_{\text{NL}}^{\text{local}}$

Band	Mask	l_{max}	$f_{\text{NL}}^{\text{local}}$	$\Delta f_{\text{NL}}^{\text{local}}$	b_{src}
V+W	KQ85	400	50 ± 29	1 ± 2	0.26 ± 1.5
V+W	KQ85	500	61 ± 26	2.5 ± 1.5	0.05 ± 0.50
V+W	KQ85	600	68 ± 31	3 ± 2	0.53 ± 0.28
V+W	KQ85	700	67 ± 31	3.5 ± 2	0.34 ± 0.20
V+W	Kp0	500	61 ± 26	2.5 ± 1.5	
V+W	KQ75p1 ^a	500	53 ± 28	4 ± 2	
V+W	KQ75	400	47 ± 32	3 ± 2	-0.50 ± 1.7
V+W	KQ75	500	55 ± 30	4 ± 2	0.15 ± 0.51
V+W	KQ75	600	61 ± 36	4 ± 2	0.53 ± 0.30
V+W	KQ75	700	58 ± 36	5 ± 2	0.38 ± 0.21

^aThis mask replaces the point-source mask in KQ75 with the one that does not mask the sources identified in the WMAP K-band data

WMAP 5-year data: 51 +/- 30
(Komatsu et al.)
more recent value: 38 +/- 21
(Smith et al.)

Why spend time on this? f_{NL} seems to be marginally inconsistent with zero. An independent check with a different statistic.

Estimators of f_{NL}

$$T(\hat{\mathbf{n}}) = \sum a_{lm} Y_l^m(\hat{\mathbf{n}}),$$

$$A_{lm}(r) \equiv \frac{\alpha_l(r)}{C_l} b_l a_{lm} \quad A(r, \hat{\mathbf{n}}) \equiv \sum_{lm} Y_{lm}(\hat{\mathbf{n}}) A_{lm}(r)$$

$$B_{lm}(r) \equiv \frac{\beta_l(r)}{C_l} b_l a_{lm} \quad B(r, \hat{\mathbf{n}}) \equiv \sum_{lm} Y_{lm}(\hat{\mathbf{n}}) B_{lm}(r),$$

$$\alpha_l(r) \equiv \frac{2}{\pi} \int k^2 dk g_{Tl}(k) j_l(kr),$$

$$\beta_l(r) \equiv \frac{2}{\pi} \int k^2 dk P_{\Phi}(k) g_{Tl}(k) j_l(kr)$$

KSW skewness (used by WMAP team)

$$S_{AB^2} \equiv \int r^2 dr \int d\hat{\mathbf{n}} A(r, \hat{\mathbf{n}}) B^2(r, \hat{\mathbf{n}})$$

Komatsu, Spergel, Wandelt 2005

Bispectrum is compressed to skewness, a single number, effectively.
Lacks any angular scale information to separate contributions.
But, easy to compute from data, easy to simulate for error estimates.
If bispectrum was primordial only, this is adequate!

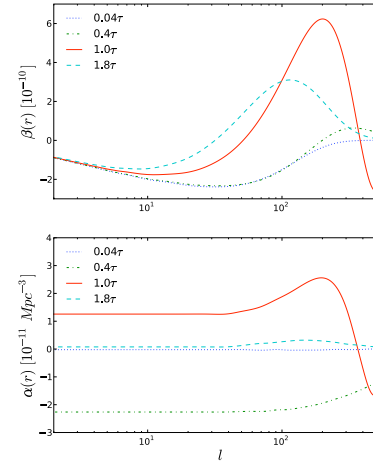
Two-to-One Power Spectrum

$$a_{lm}^2 = \int d\hat{\mathbf{n}} T^2(\hat{\mathbf{n}}) Y_l^{m*}(\hat{\mathbf{n}}) \quad C_l^{2-1} = \frac{1}{2l+1} \sum_m a_{lm}^2 a_{lm}^*$$

$$C_l^{2-1} = \frac{1}{2l+1} \sum_{l_1 l_2} B_{l_1 l_2 l}$$

$$\times \begin{pmatrix} l_1 & l_2 & l \\ 0 & 0 & 0 \end{pmatrix} \sqrt{\frac{(2l_1+1)(2l_2+1)(2l+1)}{4\pi}}$$

Cooray 2001; used by Szapudi & Chen 2006 to get $f_{NL}=22 \pm 52$ with WMAP 3-year data



Estimators of f_{NL}

$$T(\hat{\mathbf{n}}) = \sum a_{lm} Y_l^m(\hat{\mathbf{n}}),$$

$$A_{lm}(r) \equiv \frac{\alpha_l(r)}{C_l} b_l a_{lm} \quad A(r, \hat{\mathbf{n}}) \equiv \sum_{lm} Y_{lm}(\hat{\mathbf{n}}) A_{lm}(r)$$

$$B_{lm}(r) \equiv \frac{\beta_l(r)}{C_l} b_l a_{lm} \quad B(r, \hat{\mathbf{n}}) \equiv \sum_{lm} Y_{lm}(\hat{\mathbf{n}}) B_{lm}(r),$$

Weighted Skewness Power Spectrum

Munshi & Heavens 2009; Smidt et al. 2009

$$(B^2)_{lm}(r) \equiv \int d\hat{\mathbf{n}} B^2(r, \hat{\mathbf{n}}) Y_{lm}(\hat{\mathbf{n}})$$

$$(AB)_{lm}(r) \equiv \int d\hat{\mathbf{n}} A(r, \hat{\mathbf{n}}) B(r, \hat{\mathbf{n}}) Y_{lm}(\hat{\mathbf{n}})$$

$$C_l^{2-1} \equiv (C_l^{A,B^2} + 2C_l^{AB,B}) \quad (30)$$

$$C_l^{A,B^2} \equiv \frac{1}{2l+1} \int r^2 dr \left[\sum_m \text{Real} \{ A_{lm}(r) (B^2)_{lm}(r) \} \right]$$

$$C_l^{B,AB} \equiv \frac{1}{2l+1} \int r^2 dr \left[\sum_m \text{Real} \{ B_{lm}(r) (AB)_{lm}(r) \} \right]$$

**Optimized for primordial non-Gaussianity
(local type)**

$$E_{lm}(r) \equiv \frac{b_l}{C_l} a_{lm}$$

$$E(\hat{\mathbf{n}}) \equiv \sum_{lm} Y_{lm}(\hat{\mathbf{n}}) E_{lm}(r)$$

$$C_l^{E,E^2} \equiv \frac{1}{2l+1} \left[\sum_m \text{Real} \{ E_{lm}(E^2)_{lm} \} \right]$$

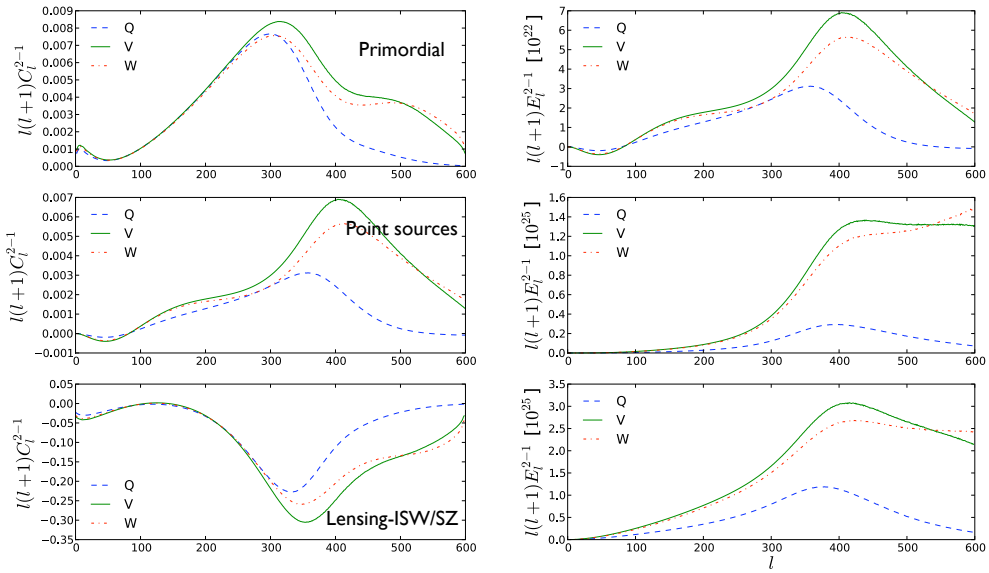
Optimized for point sources

KSW skewness:

$$\hat{S}_{AB^2} = \sum (2l+1) C_l^{2-1}$$

Theoretical Expectation

Non-Gaussianities generated from a variety of sources
(secondaries, foregrounds etc)



WMAP 5-year analysis

Practical issues:

cut-sky due to mask
 (we correct with linear terms
 in the same manner KSW skewness
 is corrected. Corrections
 are only significant at $l < 20$)

$$C_l^{2-1} = \frac{1}{f_{sky}} \left\{ C_l^{A,B^2} - 2C_l^{(A,B)B} - C_l^{A,(B^2)} \right\} + \frac{2}{f_{sky}} \left\{ C_l^{AB,B} - C_l^{(AB),B} - C_l^{B(A,B)} - C_l^{A(B,B)} \right\}$$

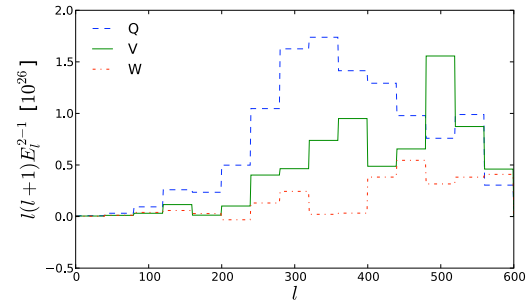
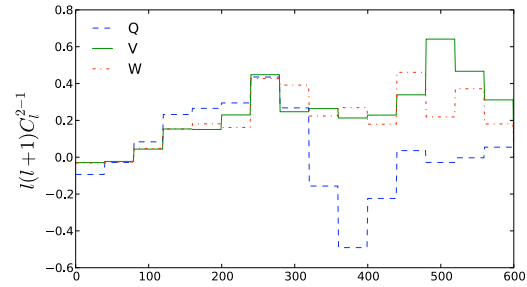
We use $l < 600$

WMAP KQ75 mask with $f_{sky}=0.718$

We present results with “raw” maps.

Our C_l/E_l fits with measurements using WMAP team’s “clean” maps have “bad” χ^2 values for the best fits.

We also think “cleaning” as done by the WMAP team creates an artificial non-Gaussianity.



WMAP 5-year analysis

Practical issues:

Error analysis

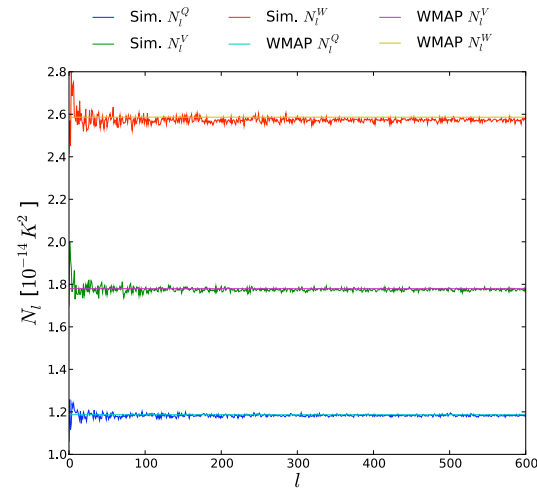
We simulate Gaussian CMB + noise maps

250 simulations per WMAP band

(Computing B_{lm}^2 , $(AB)_{lm}$, E_{lm}^2 is the most time consuming for us; it takes us ~ 5 days for $250 \times 3 \times 2$ simulations with 56 processors @ 3 GHz/each)

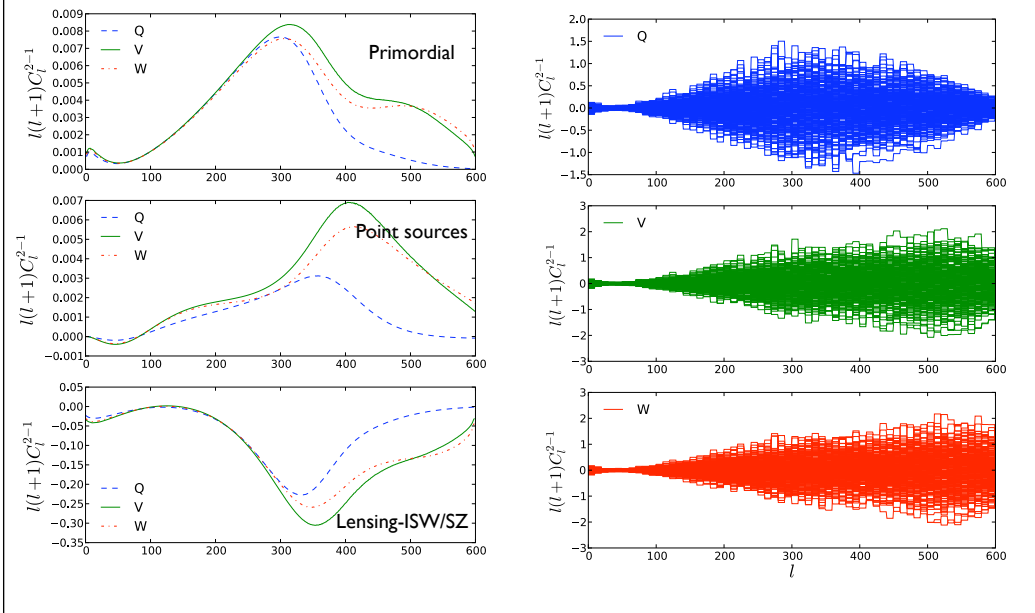
At the end, we compute the full covariance matrix:

$\text{Cov}(l_i, l_j, V_i, V_j, C_l, E_l)$



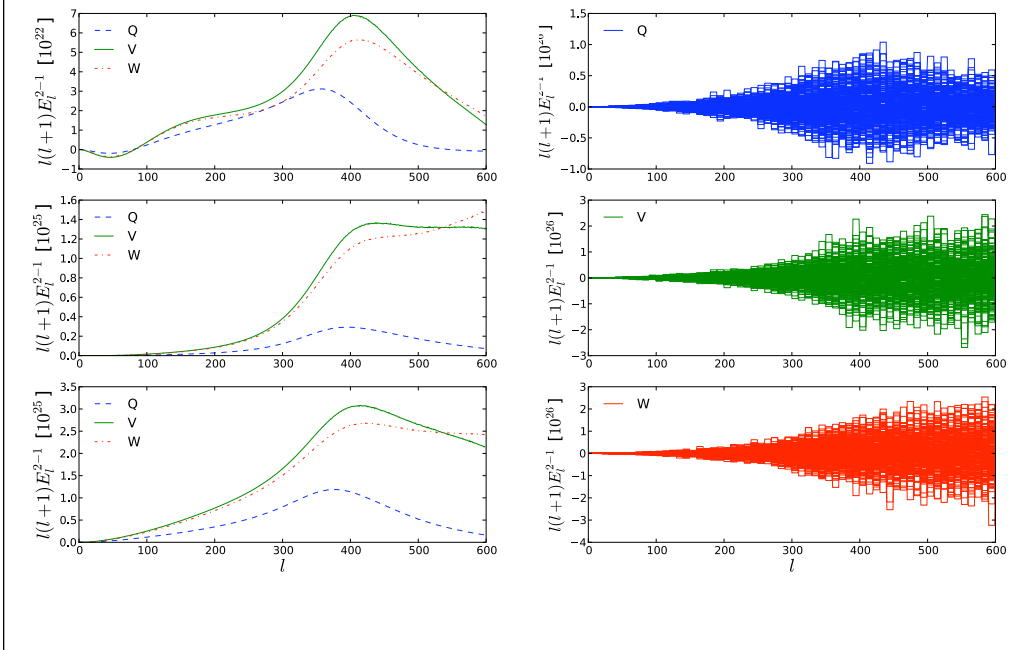
Theory Expectation vs. Data Expectation

$$C_l^{2-1}$$



Theory Expectation vs. Data Expectation

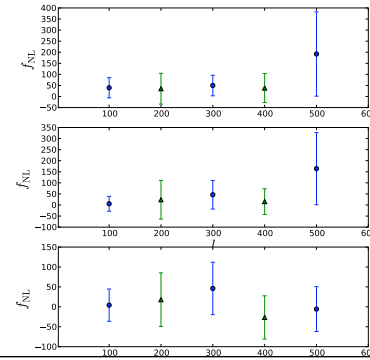
$$E_l^{2-1}$$



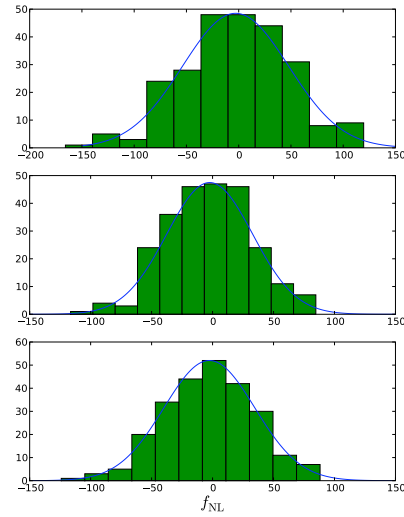
Results from WMAP 5-year analysis

Type	f_{NL} (PS + lensing)	A_Q	A_V	A_W	η_Q	η_V	η_W	χ^2/dof
C_l^{2-1}								
Q	21.1 ± 40.3	-80.2 ± 39.3			-11.7 ± 5.8			3.4
V	15.7 ± 38.9		8.7 ± 23.0			-3.7 ± 4.6		1.0
W	-13.5 ± 39.8			39.7 ± 25.6			0.6 ± 4.4	1.2
V+W	14.3 ± 37.6		18.2 ± 20.8	9.0 ± 22.0		-2.7 ± 4.1	-2.2 ± 4.0	1.3
E_l^{2-1}								
Q	122.2 ± 118.6	8.5 ± 6.2			6.6 ± 1.7			0.7
V	80.5 ± 107.8		2.1 ± 2.6			1.2 ± 1.1		0.3
W	62.3 ± 113.2			-0.2 ± 2.5			0.9 ± 1.3	0.3
V+W	72.0 ± 103.1		1.9 ± 2.4	-0.5 ± 2.4		1.4 ± 1.1	1.3 ± 1.2	0.8
Full								
Q	21.8 ± 29.6	24.0 ± 5.7			0.2 ± 1.2			3.3
V	16.7 ± 27.1		4.1 ± 2.4			0.2 ± 0.5		0.6
W	18.7 ± 27.2			0.5 ± 2.3			-0.3 ± 1.0	0.8
V+W	11.0 ± 23.7		2.8 ± 2.2	-0.4 ± 2.2		1.0 ± 0.8	-0.6 ± 0.9	0.9

Type	f_{NL} (with PSs)	f_{NL} (PSs + lensing-secondary)
C_l^{2-1}		
$2 < l < 200$	39.5 ± 45.6	5.5 ± 33.4
$100 < l < 300$	35.3 ± 69.6	23.9 ± 87.3
$200 < l < 400$	49.6 ± 46.5	46.3 ± 64.5
$300 < l < 500$	38.3 ± 65.6	15.5 ± 57.8
$400 < l < 600$	192.0 ± 190.4	164.1 ± 162.9
Full		
$2 < l < 200$	-9.2246 ± 44.6	4.2 ± 40.5
$100 < l < 300$	-6.1 ± 101.4	18.0 ± 67.2
$200 < l < 400$	64.5 ± 74.0	46.1 ± 65.8
$300 < l < 500$	68.3 ± 92.8	-26.5 ± 54.2
$400 < l < 600$	103.6 ± 178.3	-5.6 ± 56.3



Comparison to WMAP 5-year Paper



$$\hat{S}_{AB^2} = \sum (2l + 1) C_l^{2-1}$$

Band	f_{NL}	WMAP 5-year
Q	-27.3 ± 50.8	-42 ± 48
V	52.0 ± 35.2	41 ± 35
W	50.5 ± 37.3	46 ± 35

best-fit higher by 0.25σ

WMAP overall 51 ± 30 (V+W)
Our overall 11.0 ± 23.7

Also our best-fit point source amplitude (including Q band) is exactly what the WMAP team found.

Comparison with other results

Technique	f_{NL}	Ref
WMAP 3-Year, Skewness	87 ± 30	[39]
WMAP 5-Year, Skewness	51 ± 30	[12]
WMAP 5-Year, Minkowski Functions	-57 ± 61	[12]
WMAP 5-year, Wavelets	31 ± 24.5	[66]
WMAP 5-year, Needlets	84 ± 40	[67]
WMAP 5-year, N-point PDF	30 ± 62	[68]
WMAP ISW-correlation	236 ± 127	[69]
Large-scale structure bias	20.5 ± 24.8	[70]
WMAP 5-Year, Optimal Estimator	38 ± 21	[40]
WMAP 5-year, Skew-power spectrum	$11.0 \pm 23.7(\pm 1.5)$	this paper

We find the primordial non-Gaussianity in the local model is fully consistent with zero. There is not even marginal evidence for a non-zero value. Our work involves an estimator that is suboptimal, however.

On going work:

1. An optimal form accounting for mode-mode correlations (ie. implementing Smith et al. corrections) - hope to complete in 3 to 4 months
2. Generalization for the equilateral model
3. Application to other bispectra, a paper related to lensing-SZ with WMAP soon